Tankyrase modulates insulin sensitivity in skeletal muscle cells by regulating the stability of GLUT4 vesicle proteins

Received for publication, November 21, 2017, and in revised form, April 5, 2018 Published, Papers in Press, April 18, 2018, DOI 10.1074/jbc.RA117.001058

Zhiduan Su[‡], **Vinita Deshpande**[‡], **David E. James**[‡§1], **and Jacqueline Stöckli**[‡2]

From the [‡]*Charles Perkins Centre, School of Life and Environmental Sciences and the* [§]*Sydney Medical School, University of Sydney, Sydney 2006, Australia*

Edited by Jeffrey E. Pessin

Tankyrase 1 and 2, members of the poly(ADP-ribose) polymerase family, have previously been shown to play a role in insulin-mediated glucose uptake in adipocytes. However, their precise mechanism of action, and their role in insulin action in other cell types, such as myocytes, remains elusive. Treatment of differentiated L6 myotubes with the small molecule tankyrase inhibitor XAV939 resulted in insulin resistance as determined by impaired insulin-stimulated glucose uptake. Proteomic analysis of XAV939-treated myotubes identified down-regulation of several glucose transporter GLUT4 storage vesicle (GSV) proteins including RAB10, VAMP8, SORT1, and GLUT4. A similar effect was observed following knockdown of tankyrase 1 in L6 myotubes. Inhibition of the proteasome using MG132 rescued GSV protein levels as well as insulin-stimulated glucose uptake in XAV939-treated L6 myotubes. These studies reveal an important role for tankyrase in maintaining the stability of key GLUT4 regulatory proteins that in turn plays a role in regulating cellular insulin sensitivity.

Insulin regulates glucose uptake into both muscle and fat cells by stimulating the movement of the facilitative glucose transporter GLUT4 from intracellular storage vesicles called GLUT4 storage vesicle (GSV)[3] to the plasma membrane (PM) (1). Insulin triggers GLUT4 translocation via the canonical phosphatidylinositol 3-kinase/Akt signal transduction pathway, including the phosphorylation of the Akt substrate AS160, a Rab GTPase-activating protein (RabGAP) that is localized to GSVs (1–5). Phosphorylation of AS160 is thought to regulate the GTP loading of the cognate Rab, RAB10, to initiate translocation of GSVs to and fusion with the PM (1, 6–8).

Detailed molecular analyses of GLUT4 translocation have focused on the molecular composition of the GSVs in which GLUT4 is stored under basal conditions. This has led to the identification of the aminopeptidase IRAP, the sorting protein sortilin that plays a key role in the biogenesis of GSVs (9–15), the v-SNAREs VAMP2, VAMP3, and VAMP8 that play a role in docking and fusion of GSVs with the PM (16–18) and several Rab GTPases including Rab10 (3).

Another protein found to be associated with GSVs via its interaction with IRAP is tankyrase (19). Tankyrase 1/2 are members of the poly(ADP-ribose)polymerases (PARPs) that catalyze poly(ADP)-ribosylation or PARsylation, a protein post-translational modification involving addition of a large number of linear and/or branched ADP-riboses onto target proteins (20). PARsylated proteins can be targeted for ubiquitination and proteasomal degradation by the E3 ubiquitin ligase RNF146 that interacts with and is allosterically activated by the PAR chain (21, 22).

Tankyrase 1/2 have been implicated in insulin-stimulated glucose uptake in adipocytes (23). Insulin enhances tankyrase activity possibly via mitogen-activated protein kinase-mediated phosphorylation (19). Tankyrase 1 knockdown or tankyrase inhibition using the broad-range PARP inhibitor PJ34 resulted in impaired insulin-stimulated GLUT4 translocation to the PM or insulin resistance in adipocytes (23). The mechanism by which tankyrase affects insulin-stimulated GLUT4 translocation has not been established (23). Furthermore, the role of tankyrase in skeletal muscle, the tissue that plays a central role in whole body insulin-mediated glucose uptake, is not known.

The development of more selective tankyrase inhibitors, such as XAV939 (24, 25), has been the focus of anti-cancer therapeutics in an effort to inhibit aberrant Wnt/β-catenin signaling (26). Tankyrase PARsylates AXIN, which is part of the β-catenin destruction complex, and targets it for degradation, thereby leading to the stabilization and activation of the β-catenin pathway (25).

In this study, we utilized XAV939 (24, 25) to inhibit tankyrase 1/2-mediated PARsylation in L6 myotubes and showed that this impaired insulin-stimulated glucose uptake. We applied label-free quantitative proteomics (27) to determine XAV939-mediated changes in the proteome and discovered that tankyrase inhibition resulted in a reduction in protein levels of a number of GSV proteins. A similar reduction in GSV proteins

This work was supported in part by National Health and Medical Research Council (NHMRC) project Grants GNT1061122 (to D. E. J.) and GNT1068469 (to J. S). The contents of the published material are solely the responsibility of the individual authors and do not reflect the view of NHMRC. The authors declare that they have no conflicts of interest with the contents of this article.

This article contains Tables S1–S5.

The MS proteomics data have been deposited at the ProteomeXchange Consortium with identifier PXD007182.

[1] NHMRC Senior Principal Research Fellow. To whom correspondence may be addressed. Tel.: 612-862-71621; E-mail: david.james@sydney.edu.au.

[2] To whom correspondence may be addressed. Tel.: 612-862-71986; E-mail: jacqueline.stoeckli@sydney.edu.au.

[3] The abbreviations used are: GSV, GLUT4 storage vesicle; PARsylation, poly(ADP)-ribosylation; PARP, poly(ADP-ribose) polymerase; PAR, poly(ADP-ribose); 2-DG, 2-deoxyglucose; TEAB, triethylammonium bicarbonate; VAMP, vesicle-associated membrane protein; SNARE, soluble NSF attachment protein receptor; HFHSD, high-fat/high-sucrose diet; GTT, glucose tolerance test; α-MEM, α-minimum essential medium; PM, plasma membrane.

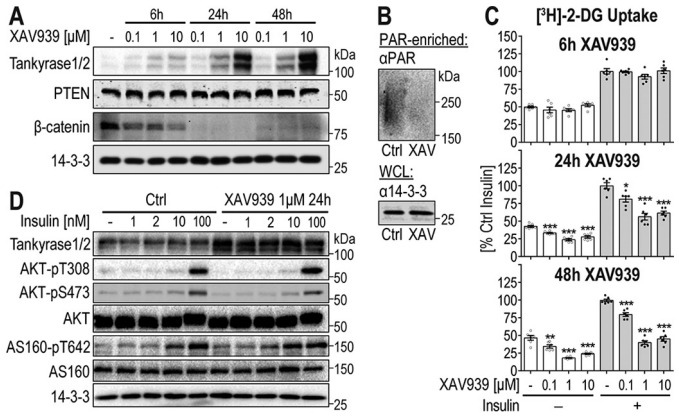

Figure 1. XAV939 treatment impaired glucose uptake in muscle. L6 myotubes were incubated with DMSO (*Ctrl*) or the indicated doses and times of XAV939 (*XAV*), followed by serum starvation and incubation with or without 100 nM insulin (*C*) or as indicated (*D*). *A,* DMSO or XAV939-treated myotubes were lysed and immunoblotted with the indicated antibodies (14-3-3 was used as a loading control). *B,* DMSO or XAV939-treated (1 μM, 24 h) myotube lysates were enriched for PARsylated proteins and subjected to immunoblotting with indicated antibodies (14-3-3 was used as a loading control in whole cell lysate (*WCL*)). *C,* DMSO or XAV939-treated cells were subjected to [^{3}H]2-DG uptake experiments. Data are mean ± S.E., $n = 6$ independent experiments; *, $p < 0.05$; **, $p < 0.01$; ***, $p < 0.001$ compared with corresponding DMSO control. *D,* DMSO or XAV939-treated myotubes were lysed and and immunoblotted with the indicated antibodies (14-3-3 was used as a loading control).

was observed when tankyrase 1 was knocked down using a tankyrase 1-specific siRNA. Proteasome inhibition reversed the XAV939-mediated effect on glucose uptake and GSV protein levels in L6 myotubes. These data show an important role for tankyrase in glucose metabolism in skeletal muscle cells and provide new insights into the mechanism of insulin resistance mediated by tankyrase dysfunction.

Results

XAV939 inhibited tankyrase activity in L6 skeletal muscle cells

To determine the role of tankyrase in glucose uptake in muscle, the small molecule tankyrase inhibitor XAV939 (24, 25) was used to inhibit tankyrase 1/2 in L6 myotubes. To confirm its efficacy in these cells, we incubated differentiated L6 myotubes with different doses of XAV939 for various times and assessed tankyrase inhibition (Fig. 1*A*). XAV939 treatment increased tankyrase 1/2 protein levels in a dose- and time-dependent manner, as previously shown (25), confirming that XAV939 inhibited tankyrase auto-PARsylation and subsequent degradation. Consistent with efficient tankyrase inhibition with XAV939 treatment, a dose- and time-dependent decrease in β-catenin protein levels was observed (Fig. 1*A*). However, PTEN abundance was not affected by XAV939 treatment in skeletal muscle cells (Fig. 1*A*), which was inconsistent with a previous study performed in cancer cell lines showing that upon tankyrase 1/2 knockdown, protein levels of the tankyrase substrate PTEN were increased (28). This suggests that regulation of PTEN protein levels may be cell type-specific. Global protein PARsylation in response to XAV939 treatment was also assessed (Fig. 1*B*). L6 myotubes were treated with or without XAV939, followed by enrichment of PARsylated proteins and immunoblotting with anti-poly(ADP-ribose) (PAR) antibodies and a decrease in global PARsylated proteins was observed with XAV939 treatment (Fig. 1*B*), confirming that XAV939 inhibits tankyrase 1/2-mediated PARsylation in skeletal muscle cells.

XAV939 treatment impaired glucose uptake

We next examined the effects of XAV939 on glucose uptake in differentiated L6 myotubes. We observed a significant dose-dependent defect in insulin-stimulated 2-deoxyglucose (2-DG) uptake after 24 and 48 h of XAV939 treatment but not after 6 h (Fig. 1*C*), indicating that tankyrase inhibition in L6 myotubes results in insulin resistance, consistent with previous reports in adipocytes (23). XAV939 treatment for 24–48 h also significantly affected basal glucose uptake in these cells. We next examined whether this defect in glucose uptake upon tankyrase inhibition was due to a defect in insulin signaling. L6 myotubes were incubated with or without XAV939 (1 μM, 24 h) and a range of insulin doses and insulin signaling was assessed by immunoblotting (Fig. 1*D*). XAV939 treatment had no effect on insulin-stimulated phosphorylation of Akt (pThr-308, pSer-473) or its substrate AS160 (pThr-642), indicating that the impairment in 2-DG uptake upon tankyrase inhibition was not due to defective insulin signaling. Taken together, these data indicate that XAV939-mediated tankyrase inhibition resulted in insulin resistance in L6 myotubes.

Proteomic analysis of tankyrase inhibition in skeletal muscle cells

To ascertain which proteins were involved in this negative regulation of glucose metabolism, we next used MS-based quantitative proteomics to study the total proteome in this cellular model. We incubated L6 myotubes with or without XAV939 (1 μM, 24 h) and subjected the samples to label-free quantitative MS analysis. This led to the identification of 4,387 proteins and quantification of 4,374 proteins (Fig. 2*A*, Table S1) using MaxQuant as described under "Experimental procedures" (27). Of these, 4,096 proteins were quantified in at least 2 replicates of both control and XAV939-treated samples (Fig. 2*A*, Table S2). The samples presented very consistent protein intensity distribution and were highly correlated (>0.98).

Data analysis revealed 103 down-regulated proteins and 104 up-regulated proteins in response to XAV939 treatment using a 1.5-fold change threshold or exclusively quantified in one condition (Tables S3 and S4). Consistent with our immunoblotting results (Fig. 1*A*), β-catenin was down-regulated (0.66-fold, p value = 0.01) in response to XAV939 treatment, and tankyrase 2 was up-regulated (only quantified in all 3 XAV939-treated samples), thereby validating the approach. We next performed gene ontology overrepresentation analysis on the 207 differentially expressed proteins. A number of biological processes were significantly enriched upon tankyrase inhibition, including "vesicle-mediated transport," which is implicated in glucose transport and GLUT4 exocytosis, the process which is defective upon tankyrase inhibition in L6 myotubes (Fig. 1*C*). Interestingly, 3 of the XAV939-regulated proteins that belong to the process "vesicle-mediated transport" are associated with GSVs (VTI1B, VAMP8, and RAB10) (3). Of particular interest were VAMP8 and RAB10, as both proteins have been shown to play an integral role in insulin-stimulated GLUT4 translocation (7,

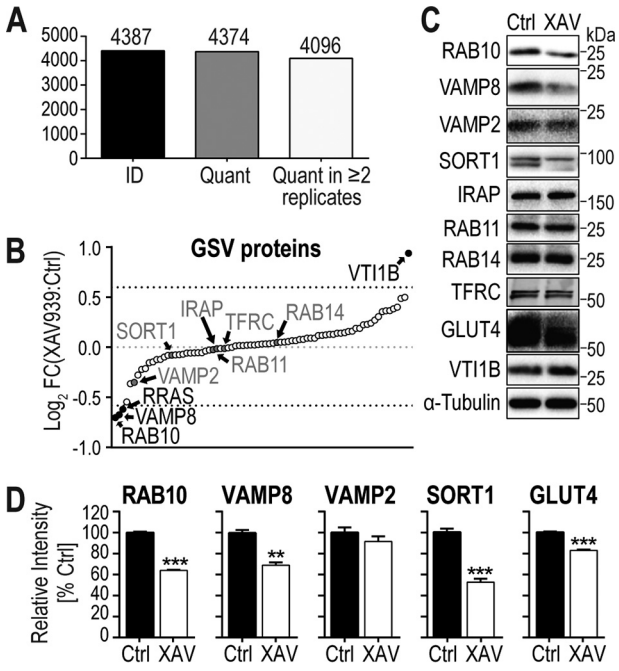

Figure 2. GSV protein analysis in response to XAV939 treatment. *A,* a total of 4,387 proteins were identified, 4,374 proteins were quantified, and 4,096 proteins were quantified in at least 2 replicates of both DMSO (*Ctrl*) and XAV939-treated (*XAV*) samples (1 μM, 24 h). *B,* XAV939-mediated Log_2 fold change (*FC*) of 79 quantified GSV proteins is shown with 1.5-fold change (*FC*) cut-off (*dotted lines* = $\pm$0.58 Log_2 FC). GSV proteins are indicated. *C,* DMSO and XAV939-treated (1 μM, 24 h) L6 myotubes were immunoblotted with the indicated antibodies (α-tubulin was used as loading control). Representative immunoblots are shown. *D,* quantification of immunoblots in *C* of the indicated proteins is shown; data are mean $\pm$ S.E., $n = 3$ independent experiments; **, $p < 0.01$; ***, $p < 0.001$ compared with Ctrl.

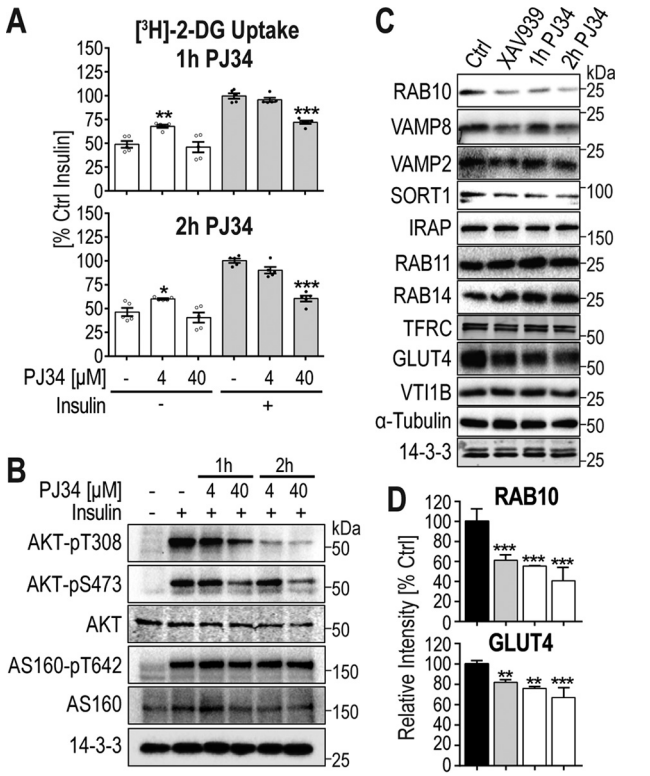

Figure 3. PJ34 treatment impaired glucose uptake and down-regulated GSV proteins in muscle. L6 myotubes were incubated with DMSO (*Ctrl*) or the indicated doses and times of PJ34, followed by serum starvation and incubation with or without 100 nM insulin. Cell were either (*A*) subjected to [^{3}H]2-DG uptake experiments or (*B* and *C*) lysed and immunoblotted with the indicated antibodies. *A,* data are mean $\pm$ S.E.; $n = 5$ independent experiments; *, <0.05; **, $p < 0.01$; ***, $p < 0.001$ compared with the corresponding DMSO control. *B* and *C,* representative immunoblots are shown. 14-3-3 and α-tubulin were used as loading controls. *C,* myotubes were treated with DMSO, 1 μM XAV939 for 24 h, or 40 μM PJ34 for 1–2 h. *D,* quantification of immunoblots in *C* of the indicated proteins is shown; data are mean $\pm$ S.D.; $n = 2$–5 independent experiments; **, $p < 0.01$; ***, $p < 0.001$ compared with Ctrl.

18, 29) and both were down-regulated upon XAV939 treatment (VAMP8, 0.63-fold and RAB10, 0.56-fold).

GSV protein analysis

Insulin triggers glucose transport in fat and muscle cells by initiating the movement of intracellular GLUT4-containing storage vesicles (GSVs) to the PM and fusion with the PM. Tankyrase inhibition resulted in impaired insulin-stimulated GLUT4 translocation in L6 myotubes (Fig. 1*C*) and it was of particular interest to observe that the protein levels of two crucial GSV proteins, VAMP8 and RAB10, were down-regulated in response to XAV939. We therefore focused our analysis on GSV proteins in the proteomics dataset. We filtered our data for previously reported GSV proteins (1, 3, 12, 30, 31) and identified 79 GSV proteins in our dataset (Fig. 2*B*, Table S5). Among these, RAB10, VAMP8, and RRAS were down-regulated and VTI1B was up-regulated in response to XAV939 treatment (Fig. 2*B*). To verify these findings and to examine additional GSV proteins not quantified by MS, we subjected control and XAV939-treated L6 myotube lysates to immunoblotting using specific antibodies for various GSV proteins. A number of crucial GSV proteins were reduced upon XAV939 treatment, including RAB10, VAMP8, SORT1, and GLUT4 (Fig. 2, *C* and *D*). Intriguingly, other *bona fide* GSV proteins, including VAMP2 and IRAP, were not modulated following inhibition of tankyrase indicating that this phenomenon was not simply *en bloc* degradation of GSVs.

Validation of the role of tankyrase on GSV protein levels in skeletal muscle cells

To validate the above findings using XAV939 we next utilized another tankyrase inhibitor, the broad-spectrum PARP inhibitor PJ34 (23). Consistent with XAV939, PJ34 (40 μM) caused an acute and significant reduction in 2-DG uptake after just 1 h of treatment and this suppression was more pronounced after 2 h (Fig. 3*A*). Insulin-stimulated Akt phosphorylation was reduced by PJ34 treatment at both Akt phosphorylation sites at a dose of 40 μM PJ34 (Fig. 3*B*). However, there was no reduction in Akt activity as assessed by phosphorylation of the Akt substrate AS160, which was not reduced by PJ34 treatment. Although it is not clear why Akt phosphorylation was affected by PJ34 treatment, these data suggest that Akt signaling was normal despite the reduction in its phosphorylation and it is likely that the residual Akt activity was sufficient as very little Akt activity is required for maximal downstream signaling (32). Notably, PJ34 treatment affected the protein levels of the GSV proteins RAB10 and GLUT4 similar to XAV939 treatment (Fig. 3, *C* and *D*).

Although XAV939 is a selective tankyrase 1/2 inhibitor, XAV939 can also bind PARP1/2 with a lesser affinity (24). We

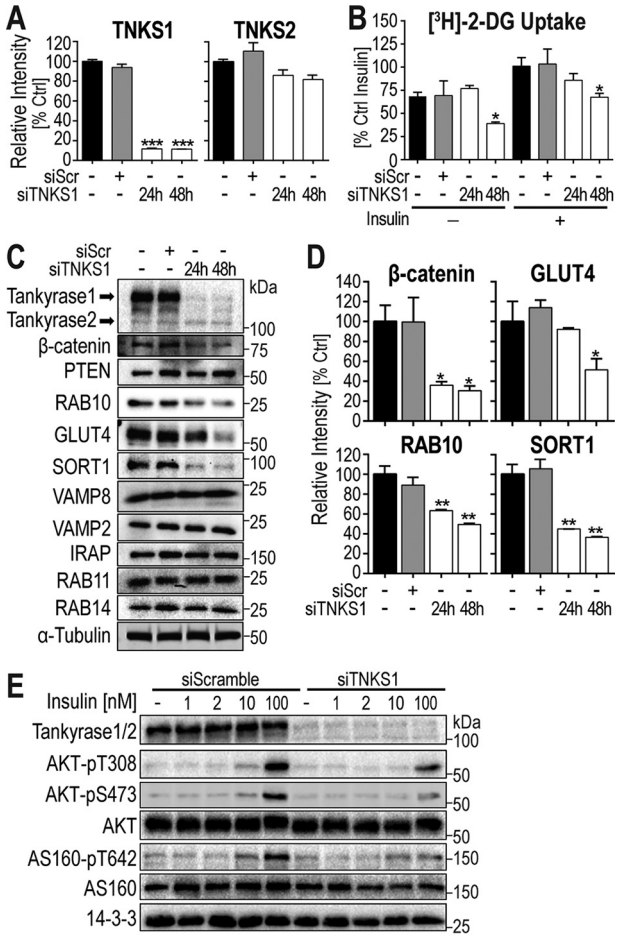

Figure 4. TNKS1 knockdown impaired glucose uptake and down-regulated GSV proteins in muscle. L6 myotubes transfected with siRNA against TNKS1 or scrambled for 24 or 48 h were either (*A* and *C*) lysed and immunoblotted or serum starved, followed by stimulation with or without 100 nM insulin (*B*) or the indicated doses of insulin (*E*) and subjected to [^{3}H]2-DG uptake experiments (*B*) or immunoblotting (*E*). Untransfected cells were used as a control (*Ctrl*). *A,* knockdown efficiency was determined. Cell lysates were immunoblotted with tankyrase antibodies and quantification of immunoblots ($n = 2$) are shown; data are mean ± S.D.; ***, $p < 0.001$. *B,* [^{3}H]2-DG uptake was assessed in Ctrl, scrambled, and TNKS1 knockdown L6 myotubes. Data are mean ± S.D.; $n = 2$ independent experiments; *, $p < 0.05$ compared with corresponding Ctrl. *C,* representative immunoblots are shown. α-Tubulin was used as a loading control. *D,* quantification of immunoblots in *C* of the indicated proteins is shown; data are mean ± S.D.; $n = 2$ independent experiments; *, $p < 0.05$; **, $p < 0.01$ compared with Ctrl. *E,* myotubes were treated and lysed 24 h after siRNA transfection and immunoblotted with the indicated antibodies. 14-3-3 was used as a loading control.

therefore tested whether the observed phenotypes in response to drug treatment were due to a specific effect on tankyrase by knocking down tankyrase 1. L6 myotubes were transfected with pooled TNKS1 siRNAs or scrambled siRNA for 24 or 48 h, resulting in efficient knockdown of TNKS1 (~90%) but not TNKS2 (Fig. 4, *A* and *C*). TNKS1 knockdown resulted in decreased β-catenin protein levels confirming that tankyrase activity was abolished and also that TNKS1 is likely the major tankyrase in L6 myotubes (Fig. 4, *C* and *D*). Basal and insulin-stimulated 2-DG uptake was significantly impaired after 48 h of TNKS1 knockdown (Fig. 4*B*), confirming that TNKS1 knockdown reproduced the results obtained with tankyrase inhibition using 2 independent drugs in L6 myotubes. Notably, the protein levels of several GSV proteins, including RAB10, GLUT4, and SORT1, were significantly reduced upon TNKS1 knockdown (Fig. 4, *C* and *D*). However, TNKS1 knockdown affected insulin signaling, resulting in reduced phosphorylation of Akt and the Akt substrate AS160 (Fig. 4*E*). Hence it is not clear whether the impairment in 2-DG uptake was due to reduced GSV proteins or defective Akt signaling or a combination of both. Nevertheless, these data confirmed an important role for tankyrase in insulin-stimulated glucose uptake and GSV protein stability in L6 myotubes. Furthermore, these data demonstrated that TNKS1, rather than TNKS2, was the key regulator for these processes.

Proteasome inhibition reversed XAV939-mediated defects in GSV protein levels and glucose uptake in skeletal muscle cells

Our data show that tankyrase inhibition affected GSV protein stability and glucose uptake in L6 myotubes. In light of the known role of tankyrase activity in proteasomal protein degradation (21, 22) we next tested the role of the proteasome in the loss of GSV proteins following inhibition of tankyrase activity. To achieve this, we utilized the proteasome inhibitor MG132 (33). MG132 treatment reversed XAV939-induced down-regulation of β-catenin as well as that of GSV proteins, including RAB10, GLUT4, SORT1, and VAMP8, indicating that proteasomal degradation was responsible for the XAV939-mediated reduction of these proteins (Fig. 5, *A* and *B*). Furthermore, 6 h of MG132 treatment also reversed the XAV939-mediated impairment in 2-DG uptake (Fig. 5*C*). Notably, treatment with MG132 alone for 6 h significantly increased GLUT4 protein levels as well as both basal and insulin-responsive glucose uptake to a similar extent to that observed with the XAV939 reversal. As expected, MG132 treatment did not affect insulin-dependent phosphorylation of Akt or AS160 (Fig. 5*D*). Furthermore, MG132 had no effect on tankyrase protein levels upon siRNA-mediated knockdown as MG132 acts post-translationally. In summary, these data suggest that glucose uptake is highly correlated to GSV protein levels and that tankyrase inhibition significantly accelerates GSV protein turnover.

Tankyrase protein levels were reduced in skeletal muscle from insulin-resistant mice

Given that tankyrase inhibition resulted in insulin resistance in L6 skeletal muscle cells, we next determined whether tankyrase levels or its activity were affected in skeletal muscle from insulin-resistant mice. C57Bl/6J mice fed a high-fat/high-sucrose diet (HFHSD) for 6 weeks were insulin-resistant as displayed by impaired glucose tolerance (Fig. 6*A*). Tankyrase 1 protein levels were significantly reduced in skeletal muscle from HFHSD-fed mice compared with chow-fed mice (Fig. 6, *B* and *C*). However, protein levels of β-catenin or GSV proteins in skeletal muscle were unaffected by the HFHSD, suggesting that the reduction in tankyrase, although significant, was not sufficient for downstream effects.

Discussion

Over the years, tankyrase has been implicated in many biological processes including carbohydrate metabolism. However, it remains unclear exactly how tankyrase mediates these effects on glucose homeostasis or if it does so in skeletal muscle.

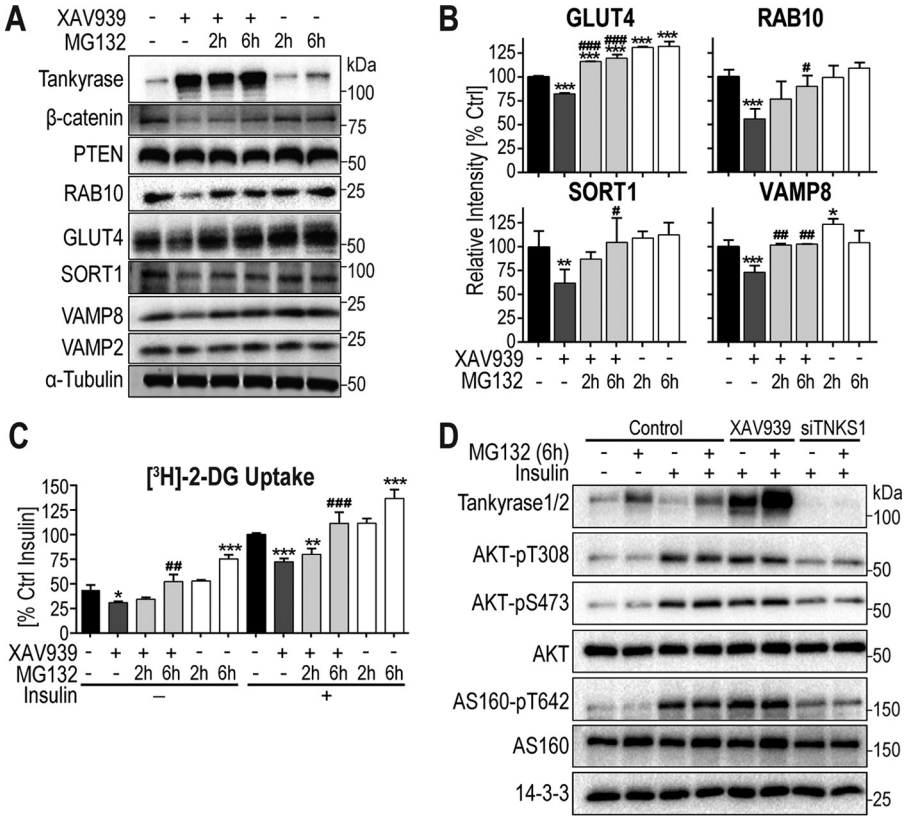

Figure 5. MG132 reversed XAV939 suppression of GSV protein levels and glucose uptake in muscle. L6 myotubes were treated with DMSO, XAV939 (1 μM, 24 h), and/or the indicated times of 10 μM MG132 and either (*A*) lysed and immunoblotted with the indicated antibodies or serum starved, followed by stimulation with or without 100 nM insulin and subjected to [^{3}H]2-DG uptake experiments (*C*) or immunoblotting (*D*). *A,* representative immunoblots are shown. α-Tubulin was used as a loading control. *B,* quantification of immunoblots in *A* of the indicated proteins is shown; data are mean ± S.D.; $n = 2$–5 independent experiments. *C,* [^{3}H]2-DG uptake was assessed; data are mean ± S.D.; $n = 2$ independent experiments. *D,* myotubes were treated as indicated (DMSO Control, 1 μM XAV939 for 24 h, TNKS1 siRNA 24 h), lysed and immunoblotted with indicated antibodies. 14-3-3 was used as a loading control. *, $p < 0.05$; **, $p < 0.01$; ***, $p < 0.001$ compared with corresponding DMSO control; #, $p < 0.05$; ##, $p < 0.01$; ###, $p < 0.001$ compared with corresponding XAV939-treated sample.

In the present study, we used two different pharmacologic inhibitors of tankyrase (XAV939, PJ34) as well as siRNA knockdown of TNKS1 to show that in L6 myotubes, tankyrase has a profound effect on regulating insulin sensitivity. Although these 3 ways of modulating tankyrase differentially affected insulin signaling, they all had in common the targeted degradation of GSV proteins that include GLUT4 itself and RAB10, and in some cases also included SORT1 and VAMP8. The proteasome appears to play a role in this effect as inhibition of the proteasome rescued the impairments in glucose uptake and GSV protein levels that were triggered upon tankyrase inhibition.

In adipocytes, PARP inhibition (PJ34) or TNKS1 knockdown also resulted in reduced insulin-stimulated GLUT4 translocation to the PM (23), indicating a similar role for tankyrase in both insulin-sensitive cell types. However, whereas in muscle cells the primary defect appeared to be on reduced levels of GSV proteins, in adipocytes there was a redistribution of GLUT4 within the cell possibly into a non-insulin–responsive compartment. One possibility that we favor is that these two mechanisms may be related. One model that explains both observations is that tankyrase activity is required to maintain the integrity or stability of GSVs by, for example, blocking their fusion with other intracellular compartments such as endosomes or lysosomes. Inhibition of tankyrase may overcome this step leading initially to redistribution of GLUT4, the principle phenotype observed in adipocytes (23), commensurate with subsequent degradation of GSV proteins, the main effect seen in muscle cells. The difference in each cell type may simply reflect differences in the kinetics of transit through these different compartments in each cell type. It was intriguing that not all GSV proteins appeared to behave in the same way in muscle cells in that IRAP and VAMP2 did not undergo tankyrase-dependent degradation indicating that certain cargo may escape sorting into the degradative pathway.

The 4 GSV proteins that showed reduced protein levels upon tankyrase inhibition in muscle all play crucial roles in GLUT4 trafficking, aside from being localized to GSVs. GLUT4 itself is obviously the most important GSV protein and responsible for insulin-stimulated glucose uptake in myotubes. The vesicle-associated membrane protein (VAMP) VAMP8 is a v-SNARE that regulates fusion of vesicles with the PM and it has previously been implicated in insulin-regulated GLUT4 trafficking in adipocytes (18). Most notably, it has been observed that simultaneous disruption in the expression of VAMP2, VAMP3, and VAMP8 is required to completely block insulin-stimulated GLUT4 translocation to the PM in adipocytes and this defect could be rescued by re-expression of any one of these three VAMPs (18), indicating an important role for VAMP8 in this process. Furthermore, whole body deletion of VAMP8 affected

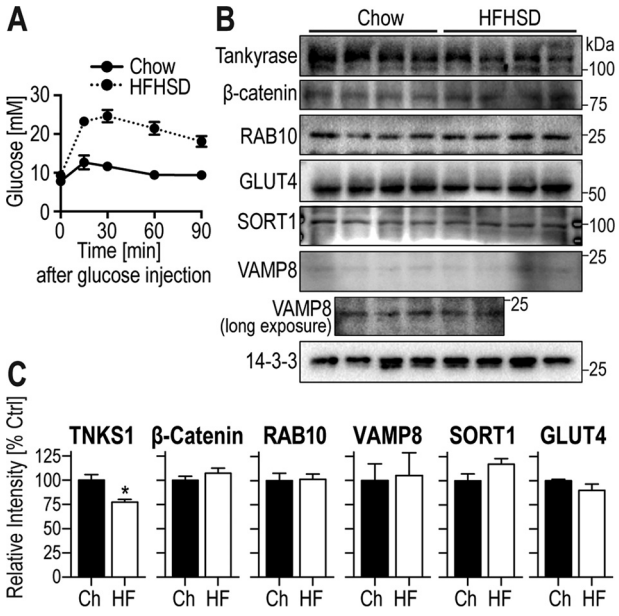

Figure 6. Tankyrase 1 protein is reduced in skeletal muscle tissue from insulin-resistant mice. C57Bl/6J mice were fed a chow diet (*Ch*) or high-fat/high-sucrose diet (HFHSD or HF) for 6 weeks. *A,* an intraperitoneal GTT at a glucose dose of 2 g/kg of lean mass was performed on the mice after 5 weeks on the diet and blood glucose was measured during the GTT. *B,* mice were euthanized after 6 weeks and skeletal muscle (quadriceps) was isolated, lysed, and immunoblotted with the indicated antibodies. 14-3-3 was used as a loading control. *C,* quantification of immunoblots in *B* of the indicated proteins is shown; data are mean ± S.E.; $n = 4$; *, $p < 0.05$ compared with chow.

glucose metabolism and glucose uptake in skeletal muscle in mice (34). RAB10 is a GTPase localized on GSVs (3) that is a substrate for the RabGAP AS160 (4) and its knockdown in adipocytes has a profound effect on insulin sensitivity (7, 8, 35). Furthermore, mice with adipose-specific deletion of RAB10 showed impaired whole body glucose homeostasis (29). Although other Rabs have been implicated in GLUT4 trafficking in L6 cells, including RAB8A, RAB13, and RAB14 (36, 37), these studies were conducted in undifferentiated myoblasts and it is possible that RAB10 only has a crucial role in differentiated cells as is the case in adipocytes (35). SORT1 has been implicated in sorting of GLUT4 into GSVs in adipocytes (11, 13) and myotubes (38) as well as GLUT4 retrograde traffic from endosomes to the trans-Golgi network thereby preventing GLUT4 traffic to lysosomes and subsequent degradation (39). So, the concerted loss of each of these proteins is likely to have a profound effect on insulin sensitivity.

It has been reported that the Wnt/β-catenin signaling pathway plays a role during myogenesis (40). Because β-catenin was markedly reduced in XAV939-treated myotubes, one possibility was that this affected myotube differentiation thereby causing the reduction in GSV protein expression. We therefore assessed whether any myogenesis or skeletal muscle proteins were changed in L6 myotubes in response to XAV939 treatment. Although some myogenesis markers were not identified in our dataset (Myf5, MyoD, and myogenin), a number of skeletal muscle-specific proteins were quantified in our dataset and were not significantly changed in response to XAV939 treatment, including skeletal muscle contractile apparatus proteins (Acta1, 1.11-fold change XAV939/control; Mylpf, 1.01; Tnni1, 1.10; Tnni2, 1.09; Tnnt3, 0.96) (41) as well as skeletal muscle glucose metabolism proteins (Gys1, 1.11; Pfkm, 1.05; Phka1, 0.90; Pygm, 0.87) (42). These data indicate that XAV939 treatment had no effect on myotube differentiation and the reduction in GSV proteins is due to direct or indirect effects of tankyrase inhibition.

One question that arises from these studies is how these GSV proteins are stabilized upon proteasome inhibition? It seems unlikely that the transmembrane domain containing GSV proteins such as GLUT4, SORT1, or VAMP8 undergo proteasomal degradation as at least GLUT4 is principally degraded via lysosomes (43, 44). One possibility is that tankyrase inhibition induces the proteasomal degradation of just one of these proteins, like RAB10, which results in the mis-targeting of all GSV proteins and their lysosomal degradation. Notably, GLUT4 protein levels are reduced upon knockdown or deletion of several cytoplasmic proteins, including AS160, its close homologue TBC1D1 and the retromer complex (39, 45, 46). In this instance, blockade of proteasomal activity would prevent degradation of these regulatory factor(s), thus overcoming this deleterious mechanism. It is unlikely that this regulatory factor is targeted for proteasomal degradation via tankyrase-mediated PARsylation because upon tankyrase inhibition the protein levels of tankyrase substrates would be increased rather than decreased. Altogether, these data suggest that the reduction in GSV protein levels upon tankyrase inhibition is likely due to an indirect effect of tankyrase inhibition involving proteasome activity. The slower reversal of insulin-regulated glucose uptake (6 h) compared with the GSV protein levels (2 h) likely reflects the slower reassembly of all GSV proteins into functional insulin-responsive vesicles, a process that may well require several hours under these conditions.

Given the prominent role of tankyrase in targeting its substrates for degradation, it was somewhat surprising that of the >200 regulated proteins identified upon XAV939 treatment, about 50% were down-regulated indicating indirect effects of tankyrase inhibition as is the case with β-catenin where upon tankyrase inhibition, its negative regulator Axin is stabilized, thereby leading to β-catenin degradation (25). Gene ontology enrichment of the XAV939-regulated proteins identified "cell proliferation" as the most significantly down-regulated process, which is consistent with the role of tankyrase in Wnt/β-catenin signaling and cell cycle, thus justifying the efforts spent on development of more specific tankyrase inhibitors for cancer treatment. Other proteins that were changed upon XAV939 treatment included proteins involved in various kinds of post-translational modifications, *e.g.* MINK1, DDRGK1, AKAP11, MNAT1, and thioredoxin2 (TXN2). Changes in their protein expression may affect the downstream signal transduction cascades via phosphorylation or redox events, implying potential cross-talk between PARsylation and other post-translational modifications. This is interesting in light of the effects of tankyrase 1 knockdown on Akt signaling, showing reduced insulin-stimulated Akt and AS160 phosphorylation. This is in contrast to 3T3-L1 adipocytes, where tankyrase 1 knockdown resulted in impaired insulin-stimulated glucose uptake in the absence of a signaling defect (23). One reason for this difference might be that L6 myotubes are less insulin sensitive than 3T3-L1 adipocytes (47, 48). Tankyrase knockdown was the only

tankyrase modulating approach that showed impaired Akt activity as neither of the inhibitors showed a defect in phosphorylation of the Akt substrate AS160. The reduction in Akt phosphorylation observed with PJ34 had no effect on Akt activity consistent with the fact that little Akt phosphorylation is required for maximal phosphorylation of Akt substrates (32). The reason for the discrepancy in insulin signaling between tankyrase inhibition and knockdown might be that in the case of the inhibitors, the tankyrase protein, whereas inactive, is still present or rather increased, suggesting that tankyrase may have activity-independent effects on insulin signaling at least in L6 myotubes. Even though the different approaches of tankyrase modulation (knockdown and 2 inhibitors) showed different effects on Akt signaling, all 3 approaches converged on insulin resistance as shown by reduced 2-DG uptake as well as a reduction in GSV protein levels, the latter being the likely cause of the observed insulin resistance upon tankyrase inhibition in these cells.

Although GLUT4 levels are reduced in adipose tissue of insulin-resistant mice as well as of humans with T2D (49, 50) this is not the case in skeletal muscle (51). Consistent with this GLUT4 protein levels were normal in insulin-resistant muscle from HFHSD-fed mice. Interestingly, tankyrase 1 protein levels were significantly reduced in insulin-resistant muscle, albeit with no effect on protein levels of GSV proteins or β-catenin, suggesting that the reduction in tankyrase 1 was not sufficient for downstream effects. Nevertheless, these data show that tankyrase 1 protein levels were impaired in insulin-resistant muscle tissue. Notably, β-catenin has previously been implicated in insulin resistance. It was part of a human skeletal muscle gene expression signature that was diagnostic for insulin resistance and inhibition of β-catenin inhibited insulin-stimulated glucose uptake in L6 myotubes (52) and in 3T3-L1 adipocytes (53). Consistent with a role for β-catenin in insulin sensitivity, drug-induced β-catenin stabilization enhances insulin-mediated glucose uptake in adipocytes (53). As β-catenin stabilization also occurs as a consequence of tankyrase activity (25), it is conceivable that tankyrase activation, which reportedly occurs in response to insulin (19), may in fact enhance insulin sensitivity. It is also possible that tankyrase activity is involved in GSV protein stabilization. Hence, it will be of interest to determine whether dysregulated β-catenin activity contributes to the altered stability of GSV proteins or if this represents a separate regulatory pathway that contributes to insulin resistance in parallel.

Taken together, this study for the first time unveils the total proteome regulation of tankyrase inhibition in skeletal muscle cells, which paves the way for expanding our knowledge of tankyrase dysfunction-induced insulin resistance. This study will also likely have an impact on the use of tankyrase inhibitors in humans as this treatment might result in insulin resistance.

Experimental procedures

Antibodies

Antibodies were purchased from Santa Cruz Biotechnology (tankyrase 1/2, 14-3-3), Trevigen (anti-PAR antibody), Sigma (TFRC, α-Tubulin), BD Biosciences Pharmingen (Vti1b), Synaptic Systems (VAMP2, VAMP8), and Cell Signaling Technology (PTEN, β-Catenin, AKT-pThr-308, AKT-pSer-473, AKT, AS160-pThr-642, RAB10). Antibodies against total AS160 (3), GLUT4 (54), and IRAP (55) were previously described. Some antibodies were kindly provided by Dr. Gus Lienhard (SORT1 (56), Dartmouth Medical School, NH), Dr. Jagath Junutula (Rab14 (57), Genentech Inc., CA), and Dr. Robert Parton (Rab11 (58), University of Queensland, Brisbane, Australia).

Cell culture and treatment

L6 rat myoblasts were grown in α-minimum essential medium (α-MEM) containing 10% fetal bovine serum in 10% CO_2 at 37 °C. L6 myoblasts were differentiated into myotubes using α-MEM with 2% fetal bovine serum when myoblasts reached 90–95% confluence. All L6 studies used myotubes between 6 and 8 days after differentiation. L6 myotubes were treated with 0.1, 1, or 10 μM XAV939 for 6, 24, or 48 h, respectively, prior to further experiments.

siRNA transfection

Three independent siRNA oligonucleotide sequences were designed against rat tankyrase 1 (Shanghai GenePharma Co., Ltd.) with the following sequences: GCAGCGAACGUGAAUGCAATT, GCGAAAGUCUACUCCGUUATT, and GCGUCGAAGUCUGUUCUUUTT. A scrambled siRNA oligonucleotide (UUCUCCGAACGUGUCACGUTT) was used as a negative control. Differentiated L6 myotubes (days 5 or 6) were transfected with TNKS1 or scrambled siRNA using Lipofectamine 2000 (Invitrogen) for 24 and 48 h, respectively, and experiments were performed on day 7 of differentiation.

PARsylated protein enrichment

PARsylated proteins were enriched as previously described (59). Briefly, cells were lysed in SDS lysis buffer (1% SDS, 10 mM HEPES, pH 8.5). Lysates were mixed with *m*-aminophenylboronic acid-agarose. After 1 h incubation at room temperature, beads were washed with SDS wash buffer (1% SDS, 100 mM HEPES, 150 mM NaCl, pH 8.5) and subsequently with wash buffer containing 100 mM HEPES and 150 mM NaCl (pH 8.5). Beads were mixed with 3 M ammonium acetate (pH 5.0) for 1.5 h and washed once with SDS lysis buffer. Beads were then incubated with 4× SDS-PAGE loading buffer at 95 °C for 10 min and the eluate was subjected to immunoblotting analysis.

SDS-PAGE and Western blotting

Protein concentrations were determined via BCA assay and 10 μg of proteins were resolved by SDS-PAGE. The gel was transferred to PVDF membranes. Membranes were blocked in 5% skim milk powder in TBST (0.1% Tween 20 in TBS) for 2 h followed by an overnight incubation at 4 °C with the indicated primary antibody solutions. Membranes were incubated with an appropriate secondary antibody at room temperature for 1 h before signals were detected using a Chemidoc. Immunoblots were quantified by ImageJ software.

[^{3}H]2-DG uptake assay

This assay was performed as previously described (30). Briefly, L6 myotubes grown in 24-well plates were serum

starved for 2 h in basal α-MEM and washed with 37 °C Krebs-Ringer buffer with 0.2% BSA. Cells were then stimulated with 100 nM insulin for 20 min in Krebs-Ringer buffer with 0.2% BSA. To determine nonspecific glucose uptake, 25 μM cytochalasin B was added to control wells prior to addition of [^{3}H]2-DG (0.125 μCi/well, 50 μM unlabeled 2-DG) during the final 5 min of insulin stimulation. Following rapid washes with ice-cold PBS, cells were solubilized in 1% Triton X-100 in PBS on a shaker for 1 h and assessed for radioactivity by scintillation counting using a β-scintillation counter. All data were normalized to protein concentration.

Mouse experiments

All experiments were approved by the University of Sydney Animal Ethics Committee. Male C57Bl/6J mice were group-housed on a 12-h light/dark cycle with free access to chow diet (13% calories from fat, 65% carbohydrate, 22% protein) or HFHSD (47% fat (7:1 lard to safflower oil ratio), 32% carbohydrate, 21% protein), and water. Mice were subjected to an intraperitoneal glucose tolerance test (GTT, 2 g/kg lean mass) after 5 weeks on either chow or HFHSD. Mice were euthanized after 6 weeks on the diet, quadriceps muscle was removed, freeze-clamped, frozen and powdered, followed by immunoblotting.

Sample preparation for MS analysis

L6 myotubes were washed with ice-cold PBS and harvested in lysis buffer (6 M urea, 2 M thiourea, 25 mM TEAB, 0.1% SDS). After sonication, cell lysates were centrifuged at 15,000 × *g* for 30 min at room temperature. The supernatant was precipitated using pre-chilled acetone overnight. Protein pellets were resuspended in buffer containing 6 M urea, 2 M thiourea, 25 mM TEAB. After reduction with 10 mM DTT at room temperature for 60 min and alkylation with 25 mM iodoacetamide at room temperature for 30 min in the dark, the protein mixture was digested using LysC (enzyme:substrate, 1:100) at 30 °C for 2 h. The protein solution was then diluted 1:5 using 25 mM TEAB and further digested with trypsin (enzyme:substrate 1:50) at 37 °C overnight. The peptide mixture was desalted using stage-tips and dried by vacuum centrifugation for total proteome analysis.

Mass spectrometry analysis and data processing

MS-based total proteome analysis was performed on a Dionex UltiMate 3000 coupled to a Q-Exactive Plus in positive polarity mode. Peptides were separated using an in-house packed 75 μm × 40-cm column (1.9 μm particle size, C18AQ) with a gradient of 10–35% acetonitrile containing 0.1% formic acid over 360 min at 250 nl/min at 55 °C. The MS1 scan was acquired from 350 to 1550 *m*/*z* (70,000 resolution, 3e6 automatic gain control, 100 ms injection time) followed by MS/MS data-dependent acquisition of the top 20 ions with higher-energy collisional dissociation (17,500 resolution, 1e5 automatic gain control, 60 ms injection time, 27 NCE, 1.2 *m*/*z* isolation width).

Raw data were processed using MaxQuant (version 1.5.3.24) (60) against a Uniprot rat database (May 2016, 37,402 entries) with default settings and minor changes. Oxidation of methionine and acetylation of protein N terminus were set as variable modifications and carbamidomethylation of cysteine was set as a fixed modification, "re-quantify," "second peptides searching," and "match between runs" were enabled. Both peptide spectral match and protein false discovery rate were set to 1%. "Label-free quantification method" (27) was used for protein quantification and normalization. The data were filtered to retain proteins quantified in at least 2 samples in each of the control and XAV939-treated conditions. Bioinformatics analysis was mainly performed using the LIMMA package (61) in the R programming environment to identify proteins differentially regulated with XAV939 treatment. Functional annotation was done by David version 6.8β (released in May 2016, https://david-d.ncifcrf.gov/)[4] (62). The MS proteomics data have been deposited at the ProteomeXchange Consortium with identifier PXD007182.

Statistical analysis

Data are presented as mean ± S.E., unless otherwise indicated. Statistical analyses were performed using *t* test or analysis of variance using GraphPad Prism software. Significance was set at $p < 0.05$ and *p* values are indicated.

Author contributions—Z. S. and V. D. data curation; Z. S., V. D., and J. S. formal analysis; Z. S. and J. S. validation; Z. S. investigation; Z. S. and J. S. visualization; Z. S. methodology; Z. S., V. D., D. E. J., and J. S. writing-original draft; Z. S., D. E. J., and J. S. project administration; Z. S., D. E. J., and J. S. writing-review and editing; D. E. J. and J. S. supervision; D. E. J. funding acquisition.

Acknowledgments—We thank Stuart Cordwell, Ben Crossett, and Angela Connolly from Mass Spectrometry Core Facility (USYD) for mass spectrometric assistance and Kristen Thomas for help with muscle tissue processing.

Note added in proof—In the version of this article that was published as a Paper in Press on April 18, 2018, the authors inadvertently omitted text specifying all antibodies used in the study, including references. This error has now been corrected.

References

1. Stöckli, J., Fazakerley, D. J., and James, D. E. (2011) GLUT4 exocytosis. *J. Cell Sci.* **124,** 4147–4159 CrossRef Medline
2. Sano, H., Kane, S., Sano, E., Miinea, C. P., Asara, J. M., Lane, W. S., Garner, C. W., and Lienhard, G. E. (2003) Insulin-stimulated phosphorylation of a Rab GTPase-activating protein regulates GLUT4 translocation. *J. Biol. Chem.* **278,** 14599–14602 CrossRef Medline
3. Larance, M., Ramm, G., Stöckli, J., van Dam, E. M., Winata, S., Wasinger, V., Simpson, F., Graham, M., Junutula, J. R., Guilhaus, M., and James, D. E. (2005) Characterization of the role of the Rab GTPase-activating protein AS160 in insulin-regulated GLUT4 trafficking. *J. Biol. Chem.* **280,** 37803–37813 CrossRef Medline
4. Miinea, C. P., Sano, H., Kane, S., Sano, E., Fukuda, M., Peränen, J., Lane, W. S., and Lienhard, G. E. (2005) AS160, the Akt substrate regulating GLUT4 translocation, has a functional Rab GTPase-activating protein domain. *Biochem. J.* **391,** 87–93 CrossRef Medline
5. Peck, G. R., Ye, S., Pham, V., Fernando, R. N., Macaulay, S. L., Chai, S. Y., and Albiston, A. L. (2006) Interaction of the Akt substrate, AS160, with the glucose transporter 4 vesicle marker protein, insulin-regulated aminopeptidase. *Mol. Endocrinol.* **20,** 2576–2583 CrossRef Medline

[4] Please note that the JBC is not responsible for the long-term archiving and maintenance of this site or any other third party hosted site.

6. Ramm, G., Larance, M., Guilhaus, M., and James, D. E. (2006) A role for 14-3-3 in insulin-stimulated GLUT4 translocation through its interaction with the RabGAP AS160. *J. Biol. Chem.* **281,** 29174–29180 CrossRef Medline
7. Sano, H., Eguez, L., Teruel, M. N., Fukuda, M., Chuang, T. D., Chavez, J. A., Lienhard, G. E., and McGraw, T. E. (2007) Rab10, a target of the AS160 Rab GAP, is required for insulin-stimulated translocation of GLUT4 to the adipocyte plasma membrane. *Cell Metab.* **5,** 293–303 CrossRef Medline
8. Sano, H., Roach, W. G., Peck, G. R., Fukuda, M., and Lienhard, G. E. (2008) Rab10 in insulin-stimulated GLUT4 translocation. *Biochem. J.* **411,** 89–95 CrossRef Medline
9. Kandror, K. V., Yu, L., and Pilch, P. F. (1994) The major protein of GLUT4-containing vesicles, gp160, has aminopeptidase activity. *J. Biol. Chem.* **269,** 30777–30780 Medline
10. Lin, B. Z., Pilch, P. F., and Kandror, K. V. (1997) Sortilin is a major protein component of Glut4-containing vesicles. *J. Biol. Chem.* **272,** 24145–24147 CrossRef Medline
11. Shi, J., and Kandror, K. V. (2005) Sortilin is essential and sufficient for the formation of Glut4 storage vesicles in 3T3-L1 adipocytes. *Dev. Cell* **9,** 99–108 CrossRef Medline
12. Jedrychowski, M. P., Gartner, C. A., Gygi, S. P., Zhou, L., Herz, J., Kandror, K. V., and Pilch, P. F. (2010) Proteomic analysis of GLUT4 storage vesicles reveals LRP1 to be an important vesicle component and target of insulin signaling. *J. Biol. Chem.* **285,** 104–114 CrossRef Medline
13. Huang, G., Buckler-Pena, D., Nauta, T., Singh, M., Asmar, A., Shi, J., Kim, J. Y., and Kandror, K. V. (2013) Insulin responsiveness of glucose transporter 4 in 3T3-L1 cells depends on the presence of sortilin. *Mol. Biol. Cell* **24,** 3115–3122 CrossRef Medline
14. Keller, S. R., Scott, H. M., Mastick, C. C., Aebersold, R., and Lienhard, G. E. (1995) Cloning and characterization of a novel insulin-regulated membrane aminopeptidase from Glut4 vesicles. *J. Biol. Chem.* **270,** 23612–23618 CrossRef Medline
15. Mastick, C. C., Aebersold, R., and Lienhard, G. E. (1994) Characterization of a major protein in GLUT4 vesicles: concentration in the vesicles and insulin-stimulated translocation to the plasma membrane. *J. Biol. Chem.* **269,** 6089–6092 Medline
16. Cain, C. C., Trimble, W. S., and Lienhard, G. E. (1992) Members of the VAMP family of synaptic vesicle proteins are components of glucose transporter-containing vesicles from rat adipocytes. *J. Biol. Chem.* **267,** 11681–11684 Medline
17. Olson, A. L., Knight, J. B., and Pessin, J. E. (1997) Syntaxin 4, VAMP2, and/or VAMP3/cellubrevin are functional target membrane and vesicle SNAP receptors for insulin-stimulated GLUT4 translocation in adipocytes. *Mol. Cell Biol.* **17,** 2425–2435 CrossRef Medline
18. Zhao, P., Yang, L., Lopez, J. A., Fan, J., Burchfield, J. G., Bai, L., Hong, W., Xu, T., and James, D. E. (2009) Variations in the requirement for v-SNAREs in GLUT4 trafficking in adipocytes. *J. Cell Sci.* **122,** 3472–3480 CrossRef Medline
19. Chi, N. W., and Lodish, H. F. (2000) Tankyrase is a golgi-associated mitogen-activated protein kinase substrate that interacts with IRAP in GLUT4 vesicles. *J. Biol. Chem.* **275,** 38437–38444 CrossRef Medline
20. Haikarainen, T., Krauss, S., and Lehtio, L. (2014) Tankyrases: structure, function and therapeutic implications in cancer. *Curr. Pharm. Des.* **20,** 6472–6488 CrossRef Medline
21. Zhang, Y., Liu, S., Mickanin, C., Feng, Y., Charlat, O., Michaud, G. A., Schirle, M., Shi, X., Hild, M., Bauer, A., Myer, V. E., Finan, P. M., Porter, J. A., Huang, S. M., and Cong, F. (2011) RNF146 is a poly(ADP-ribose)-directed E3 ligase that regulates axin degradation and Wnt signalling. *Nat. Cell Biol.* **13,** 623–629 CrossRef Medline
22. DaRosa, P. A., Wang, Z., Jiang, X., Pruneda, J. N., Cong, F., Klevit, R. E., and Xu, W. (2015) Allosteric activation of the RNF146 ubiquitin ligase by a poly(ADP-ribosyl)ation signal. *Nature* **517,** 223–226 CrossRef Medline
23. Yeh, T. Y., Sbodio, J. I., Tsun, Z. Y., Luo, B., and Chi, N. W. (2007) Insulin-stimulated exocytosis of GLUT4 is enhanced by IRAP and its partner tankyrase. *Biochem. J.* **402,** 279–290 CrossRef Medline
24. Wahlberg, E., Karlberg, T., Kouznetsova, E., Markova, N., Macchiarulo, A., Thorsell, A. G., Pol, E., Frostell, Å., Ekblad, T., Öncü, D., Kull, B., Robertson, G. M., Pellicciari, R., Schüler, H., and Weigelt, J. (2012) Family-wide chemical profiling and structural analysis of PARP and tankyrase inhibitors. *Nat. Biotechnol.* **30,** 283–288 CrossRef Medline
25. Huang, S. M., Mishina, Y. M., Liu, S., Cheung, A., Stegmeier, F., Michaud, G. A., Charlat, O., Wiellette, E., Zhang, Y., Wiessner, S., Hild, M., Shi, X., Wilson, C. J., Mickanin, C., Myer, V., *et al.* (2009) Tankyrase inhibition stabilizes axin and antagonizes Wnt signalling. *Nature* **461,** 614–620 CrossRef Medline
26. Thorvaldsen, T. E. (2017) Targeting tankyrase to fight WNT-dependent tumours. *Basic Clin. Pharmacol. Toxicol.* **121,** 81–88 CrossRef Medline
27. Cox, J., Hein, M. Y., Luber, C. A., Paron, I., Nagaraj, N., and Mann, M. (2014) Accurate proteome-wide label-free quantification by delayed normalization and maximal peptide ratio extraction, termed MaxLFQ. *Mol. Cell. Proteomics* **13,** 2513–2526 CrossRef Medline
28. Li, N., Zhang, Y., Han, X., Liang, K., Wang, J., Feng, L., Wang, W., Songyang, Z., Lin, C., Yang, L., Yu, Y., and Chen, J. (2015) Poly-ADP ribosylation of PTEN by tankyrases promotes PTEN degradation and tumor growth. *Genes Dev.* **29,** 157–170 CrossRef Medline
29. Vazirani, R. P., Verma, A., Sadacca, L. A., Buckman, M. S., Picatoste, B., Beg, M., Torsitano, C., Bruno, J. H., Patel, R. T., Simonyte, K., Camporez, J. P., Moreira, G., Falcone, D. J., Accili, D., Elemento, O., Shulman, G. I., Kahn, B. B., and McGraw, T. E. (2016) Disruption of adipose Rab10-dependent insulin signaling causes hepatic insulin resistance. *Diabetes* **65,** 1577–1589 CrossRef Medline
30. Fazakerley, D. J., Naghiloo, S., Chaudhuri, R., Koumanov, F., Burchfield, J. G., Thomas, K. C., Krycer, J. R., Prior, M. J., Parker, B. L., Murrow, B. A., Stöckli, J., Meoli, C. C., Holman, G. D., and James, D. E. (2015) Proteomic analysis of GLUT4 storage vesicles reveals tumor suppressor candidate 5 (TUSC5) as a novel regulator of insulin action in adipocytes. *J. Biol. Chem.* **290,** 23528–23542 CrossRef Medline
31. Hashiramoto, M., and James, D. E. (2000) Characterization of insulin-responsive GLUT4 storage vesicles isolated from 3T3-L1 adipocytes. *Mol. Cell Biol.* **20,** 416–427 CrossRef Medline
32. Tan, S. X., Ng, Y., Meoli, C. C., Kumar, A., Khoo, P. S., Fazakerley, D. J., Junutula, J. R., Vali, S., James, D. E., and Stöckli, J. (2012) Amplification and demultiplexing in the insulin-regulated Akt pathway in adipocytes. *J. Biol. Chem.* **287,** 6128–6138 CrossRef Medline
33. Lee, D. H., and Goldberg, A. L. (1998) Proteasome inhibitors: valuable new tools for cell biologists. *Trends Cell Biol.* **8,** 397–403 CrossRef Medline
34. Zong, H., Wang, C. C., Vaitheesvaran, B., Kurland, I. J., Hong, W., and Pessin, J. E. (2011) Enhanced energy expenditure, glucose utilization, and insulin sensitivity in VAMP8 null mice. *Diabetes* **60,** 30–38 CrossRef Medline
35. Brewer, P. D., Habtemichael, E. N., Romenskaia, I., Mastick, C. C., and Coster, A. C. (2016) Glut4 is sorted from a Rab10 GTPase-independent constitutive recycling pathway into a highly insulin-responsive Rab10 GTPase-dependent sequestration pathway after adipocyte differentiation. *J. Biol. Chem.* **291,** 773–789 CrossRef Medline
36. Ishikura, S., Bilan, P. J., and Klip, A. (2007) Rabs 8A and 14 are targets of the insulin-regulated Rab-GAP AS160 regulating GLUT4 traffic in muscle cells. *Biochem. Biophys. Res. Commun.* **353,** 1074–1079 CrossRef Medline
37. Sun, Y., Bilan, P. J., Liu, Z., and Klip, A. (2010) Rab8A and Rab13 are activated by insulin and regulate GLUT4 translocation in muscle cells. *Proc. Natl. Acad. Sci. U.S.A.* **107,** 19909–19914 CrossRef Medline
38. Tsuchiya, Y., Hatakeyama, H., Emoto, N., Wagatsuma, F., Matsushita, S., and Kanzaki, M. (2010) Palmitate-induced down-regulation of sortilin and impaired GLUT4 trafficking in C2C12 myotubes. *J. Biol. Chem.* **285,** 34371–34381 CrossRef Medline
39. Pan, X., Zaarur, N., Singh, M., Morin, P., and Kandror, K. V. (2017) Sortilin and retromer mediate retrograde transport of Glut4 in 3T3-L1 adipocytes. *Mol. Biol. Cell* **28,** 1667–1675 CrossRef Medline
40. Cisternas, P., Henriquez, J. P., Brandan, E., and Inestrosa, N. C. (2014) Wnt signaling in skeletal muscle dynamics: myogenesis, neuromuscular synapse and fibrosis. *Mol. Neurobiol.* **49,** 574–589 CrossRef Medline
41. Holland, A., and Ohlendieck, K. (2013) Proteomic profiling of the contractile apparatus from skeletal muscle. *Expert Rev. Proteomics* **10,** 239–257 CrossRef Medline

42. Adeva-Andany, M. M., González-Lucan, M., Donapetry-García, C., Fernández-Fernández, C., and Ameneiros-Rodríguez, E. (2016) Glycogen metabolism in humans. *BBA Clin.* **5,** 85–100 CrossRef Medline
43. Ma, J., Nakagawa, Y., Kojima, I., and Shibata, H. (2014) Prolonged insulin stimulation down-regulates GLUT4 through oxidative stress-mediated retromer inhibition by a protein kinase CK2-dependent mechanism in 3T3-L1 adipocytes. *J. Biol. Chem.* **289,** 133–142 CrossRef Medline
44. Xie, B., Chen, Q., Chen, L., Sheng, Y., Wang, H. Y., and Chen, S. (2016) The inactivation of RabGAP function of AS160 promotes lysosomal degradation of GLUT4 and causes postprandial hyperglycemia and hyperinsulinemia. *Diabetes* **65,** 3327–3340 CrossRef Medline
45. Stöckli, J., Meoli, C. C., Hoffman, N. J., Fazakerley, D. J., Pant, H., Cleasby, M. E., Ma, X., Kleinert, M., Brandon, A. E., Lopez, J. A., Cooney, G. J., and James, D. E. (2015) The RabGAP TBC1D1 plays a central role in exercise-regulated glucose metabolism in skeletal muscle. *Diabetes* **64,** 1914–1922 CrossRef Medline
46. Lansey, M. N., Walker, N. N., Hargett, S. R., Stevens, J. R., and Keller, S. R. (2012) Deletion of Rab GAP AS160 modifies glucose uptake and GLUT4 translocation in primary skeletal muscles and adipocytes and impairs glucose homeostasis. *Am. J. Physiol. Endocrinol. Metab.* **303,** E1273–1286 CrossRef Medline
47. Robinson, R., Robinson, L. J., James, D. E., and Lawrence, J. C., Jr. (1993) Glucose transport in L6 myoblasts overexpressing GLUT1 and GLUT4. *J. Biol. Chem.* **268,** 22119–22126 Medline
48. Ng, Y., Ramm, G., Burchfield, J. G., Coster, A. C., Stöckli, J., and James, D. E. (2010) Cluster analysis of insulin action in adipocytes reveals a key role for Akt at the plasma membrane. *J. Biol. Chem.* **285,** 2245–2257 CrossRef Medline
49. Pedersen, O., Kahn, C. R., Flier, J. S., and Kahn, B. B. (1991) High fat feeding causes insulin resistance and a marked decrease in the expression of glucose transporters (Glut 4) in fat cells of rats. *Endocrinology* **129,** 771–777 CrossRef Medline
50. Sinha, M. K., Raineri-Maldonado, C., Buchanan, C., Pories, W. J., Carter-Su, C., Pilch, P. F., and Caro, J. F. (1991) Adipose tissue glucose transporters in NIDDM: decreased levels of muscle/fat isoform. *Diabetes* **40,** 472–477 CrossRef Medline
51. Pedersen, O., Bak, J. F., Andersen, P. H., Lund, S., Moller, D. E., Flier, J. S., and Kahn, B. B. (1990) Evidence against altered expression of GLUT1 or GLUT4 in skeletal muscle of patients with obesity or NIDDM. *Diabetes* **39,** 865–870 CrossRef Medline
52. Chaudhuri, R., Khoo, P. S., Tonks, K., Junutula, J. R., Kolumam, G., Modrusan, Z., Samocha-Bonet, D., Meoli, C. C., Hocking, S., Fazakerley, D. J., Stöckli, J., Hoehn, K. L., Greenfield, J. R., Yang, J. Y. H., and James, D. E. (2015) Cross-species gene expression analysis identifies a novel set of genes implicated in human insulin sensitivity. *Npj. Syst. Biol. Appl.* **1,** 15010 CrossRef Medline
53. Dissanayake, W. C., Sorrenson, B., Cognard, E., Hughes, W. E., and Shepherd, P. R. (2018) β-Catenin is important for the development of an insulin responsive pool of GLUT4 glucose transporters in 3T3-L1 adipocytes. *Exp. Cell Res.* **366,** 49–54 CrossRef Medline
54. James, D. E., Brown, R., Navarro, J., and Pilch, P. F. (1988) Insulin-regulatable tissues express a unique insulin-sensitive glucose transport protein. *Nature* **333**, 183–185 CrossRef Medline
55. Shewan, A. M., van Dam, E. M., Martin, S., Luen, T. B., Hong, W., Bryant, N. J., and James, D. E. (2003) GLUT4 recycles via a trans-Golgi network (TGN) subdomain enriched in Syntaxins 6 and 16 but not TGN38: involvement of an acidic targeting motif. *Mol. Biol. Cell* **14**, 973–986 CrossRef Medline
56. Morris, N. J., Ross, S. A., Lane, W. S., Moestrup, S. K., Petersen, C. M., Keller, S. R., and Lienhard, G. E. (1998) Sortilin is the major 110-kDa protein in GLUT4 vesicles from adipocytes. *J. Biol. Chem.* **273**, 3582–3587 CrossRef Medline
57. Junutula, J. R., De Maziére, A. M., Peden, A. A., Ervin, K. E., Advani, R. J., van Dijk, S. M., Klumperman, J., and Scheller, R. H. (2004) Rab14 is involved in membrane trafficking between the Golgi complex and endosomes. *Mol. Biol. Cell* **15**, 2218–2229 CrossRef Medline
58. Urbé, S., Huber, L. A., Zerial, M., Tooze, S. A., and Parton, R. G. (1993) Rab11, a small GTPase associated with both constitutive and regulated secretory pathways in PC12 cells. *FEBS Lett.* **334**, 175–182 CrossRef Medline
59. Zhang, Y., Wang, J., Ding, M., and Yu, Y. (2013) Site-specific characterization of the Asp- and Glu-ADP-ribosylated proteome. *Nat. Methods* **10,** 981–984 CrossRef Medline
60. Cox, J., and Mann, M. (2008) MaxQuant enables high peptide identification rates, individualized p.p.b.-range mass accuracies and proteome-wide protein quantification. *Nat. Biotechnol.* **26,** 1367–1372 CrossRef Medline
61. Ritchie, M. E., Phipson, B., Wu, D., Hu, Y., Law, C. W., Shi, W., and Smyth, G. K. (2015) limma powers differential expression analyses for RNA-sequencing and microarray studies. *Nucleic Acids Res.* **43,** e47 CrossRef Medline
62. Huang da, W., Sherman, B. T., and Lempicki, R. A. (2009) Systematic and integrative analysis of large gene lists using DAVID bioinformatics resources. *Nat. Protoc.* **4,** 44–57 CrossRef Medline